[Journal of Geophysical Research-Space]

Supporting Information for

Rapid Outer Radiation Belt Flux Dropouts and Fast Acceleration during the March 2015 and 2013 Storms: The Role of ULF Wave Transport from a Dynamic Outer Boundary

L. G. Ozeke[1], I. R. Mann[1], S. K. Y. Dufresne[1], L. Olifer[1], S. K. Morley[2], S. G. Claudepierre[3,4], K. R. Murphy[5], H. E. Spence[6], D. N. Baker[7] and A. W. Degeling[8]

[1]Department of Physics, University of Alberta, Edmonton, Alberta, Canada

[2]Los Alamos National Laboratory, Los Alamos, New Mexico, USA

[3]Space Sciences Department, The Aerospace Corporation, Los Angeles, California, USA

[4]Department of Atmospheric and Oceanic Sciences, University of California, Los Angeles, CA, USA

[5]NASA Goddard Spaceflight Center, Code 674, Greenbelt, Maryland, MD 20771, USA

[6]Institute for the Study of Earth, Oceans, and Space, University of New Hampshire, Durham, New Hampshire, USA

[7]Laboratory for Atmospheric and Space Physics, University of Colorado Boulder, Boulder, Colorado, USA

[8]Institute of Space Science, Shandong University, Weihai, China

Correspondence to: L. G. Ozeke (lozeke@ualberta.ca)

Contents of this file

Supporting Figures S1, S2, S3, S4, S5 and S6, including a brief explanation of their content as a supplement to the results and conclusions drawn in the main article.

Introduction

Results showing the pitch-angle distribution during the March 2015 and March 2013 flux dropout intervals in the same format as Figure 2 in the main article except for 1.0 MeV energy electrons instead of for 1.9 MeV energy electrons, are presented in supporting Figure S1. Figure S2 shows the time interval where the last closed drift (LCDS) drops below L^*=5 during the March 2015 and 2013 storms, indicating that at these times electrons at L^*>5 would be lost to the magnetopause. The results presented in Figure S2 are used to specify the times where the outer boundary condition at L^*=5 in the simulation results presented in the main article are set to zero. Figure S3 shows the location of the plasmapause used to separate the regions where plasmaspheric hiss loss and chorus loss are applied in the simulations presented in the main article. Figure S4 is the same as Figure 4 in the main article except during the flux dropout interval the outer boundary where the flux is set to zero is moved inward to L^*=4. Figures S5 and S6 show the evolution of the electron phase space density in the same format and at the same K-value as shown in Figure 9 in the main article except at first adiabatic invariants of 1590 MeV/G and 3980 MeV/G instead of 2750 MeV/G.

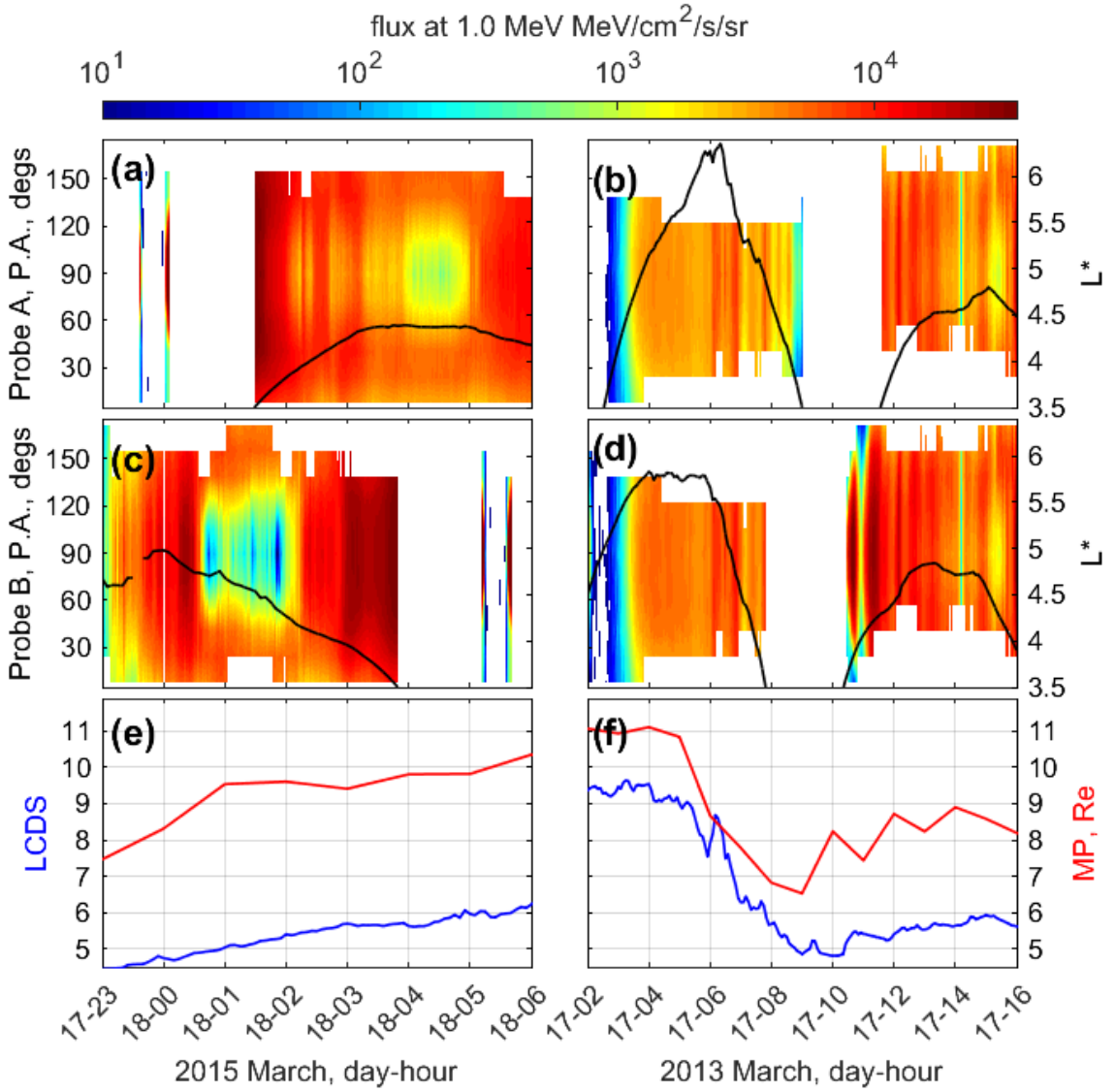

Figure S1: Panels (a) – (d) show the pitch angle, P. A. distributions of the 1.0 MeV electron flux measured by the Van Allan Probes during the March 2015 (left panels) and March 2013 (right panels) flux dropouts. The red curves in panels (e) and (f) show the location of the magnetopause MP, derived using the Shue et al. (1998) model, the blue curves show the location of the last close drift shell LCDS.

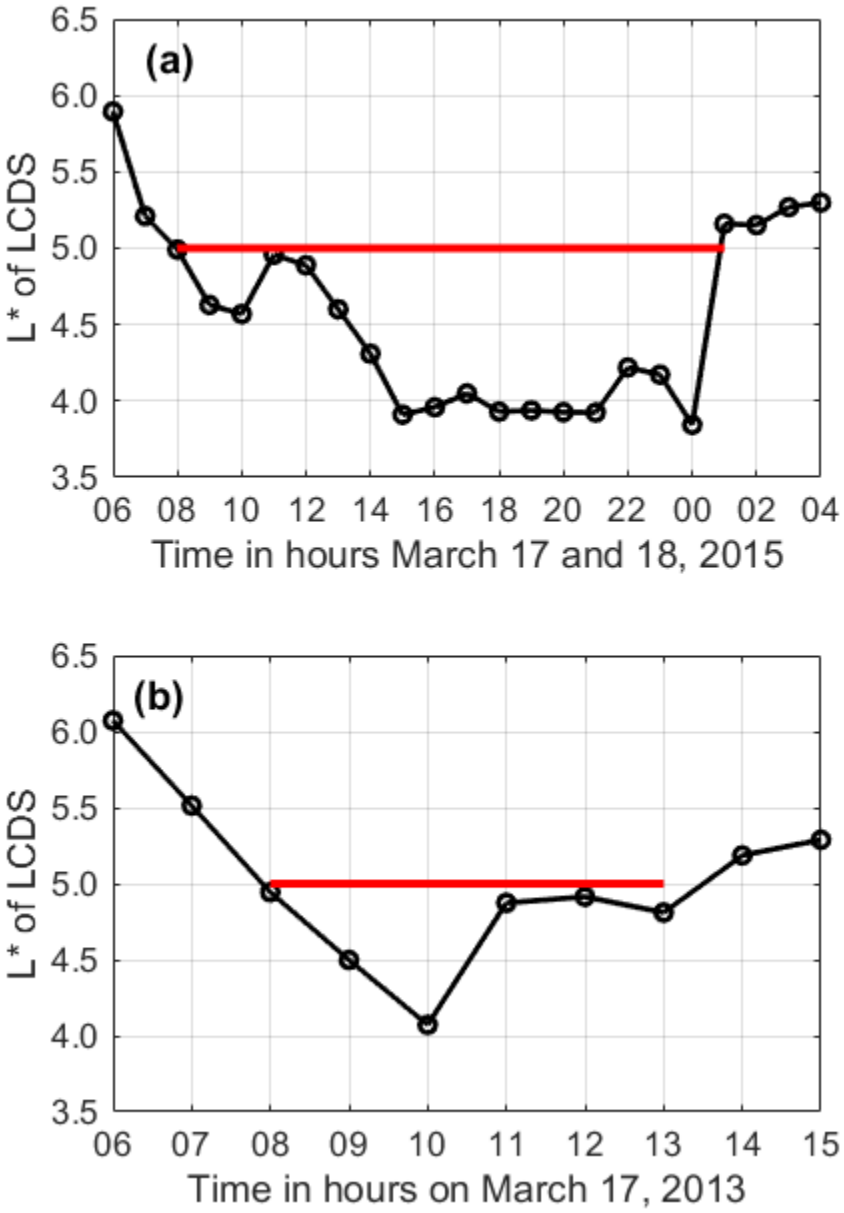

Figure S2: Hourly averaged *L values of the last closed drift shells (LCDS) during the March 2015 (a) and March 2013 (b) geomagnetic storms. The LCDS was derived at K=0.05 $G^{1/2}Re$ using the TS04 Tsyganenko and Sitnov (2005) model and the LANLGeoMag software library (Henderson et al., 2017). The time intervals highlighted in red indicates the times where the LCDS dropped below *L** of 5, the location of the outer boundary condition used for the simulations presented Figures 4, 5, 6, 7 and 8 in the main article. At these times the outer boundary condition used in the simulations was set to zero, representing electron loss to the magnetopause.**

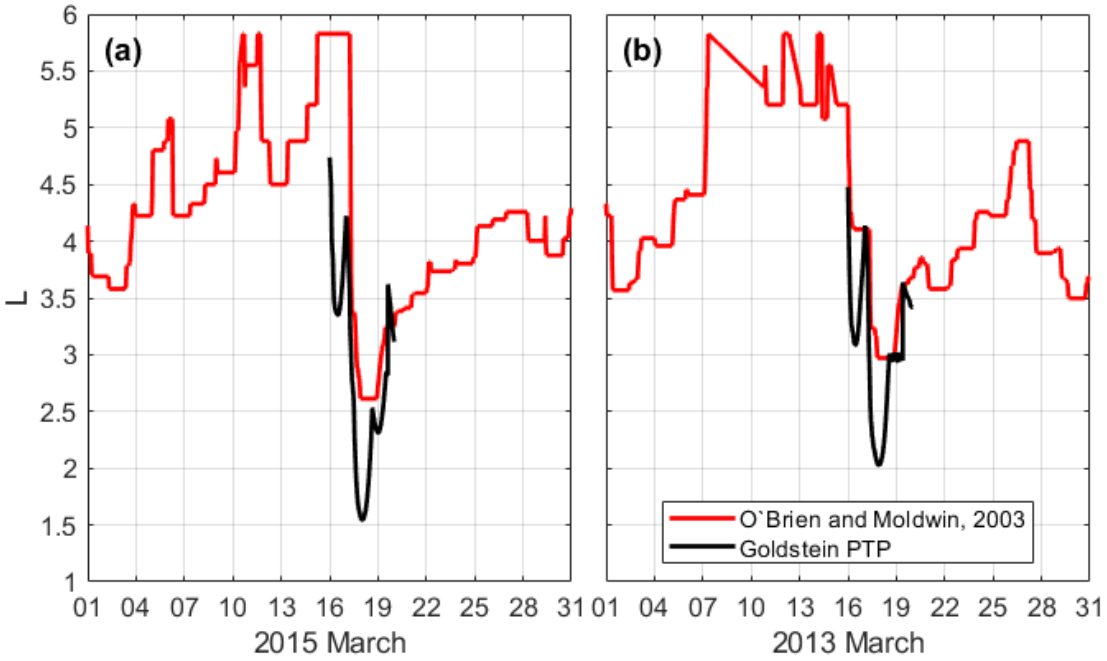

Figure S3: L-shell location of the plasmapause during the March 2015 (a) and March 2013 (b) storms derived using the empirical O'Brien and Moldwin (2003) model as a function of the Dst index and the plasmapause test particle (PTP) simulation output presented in Goldstein et al. (2014a, 2014b).

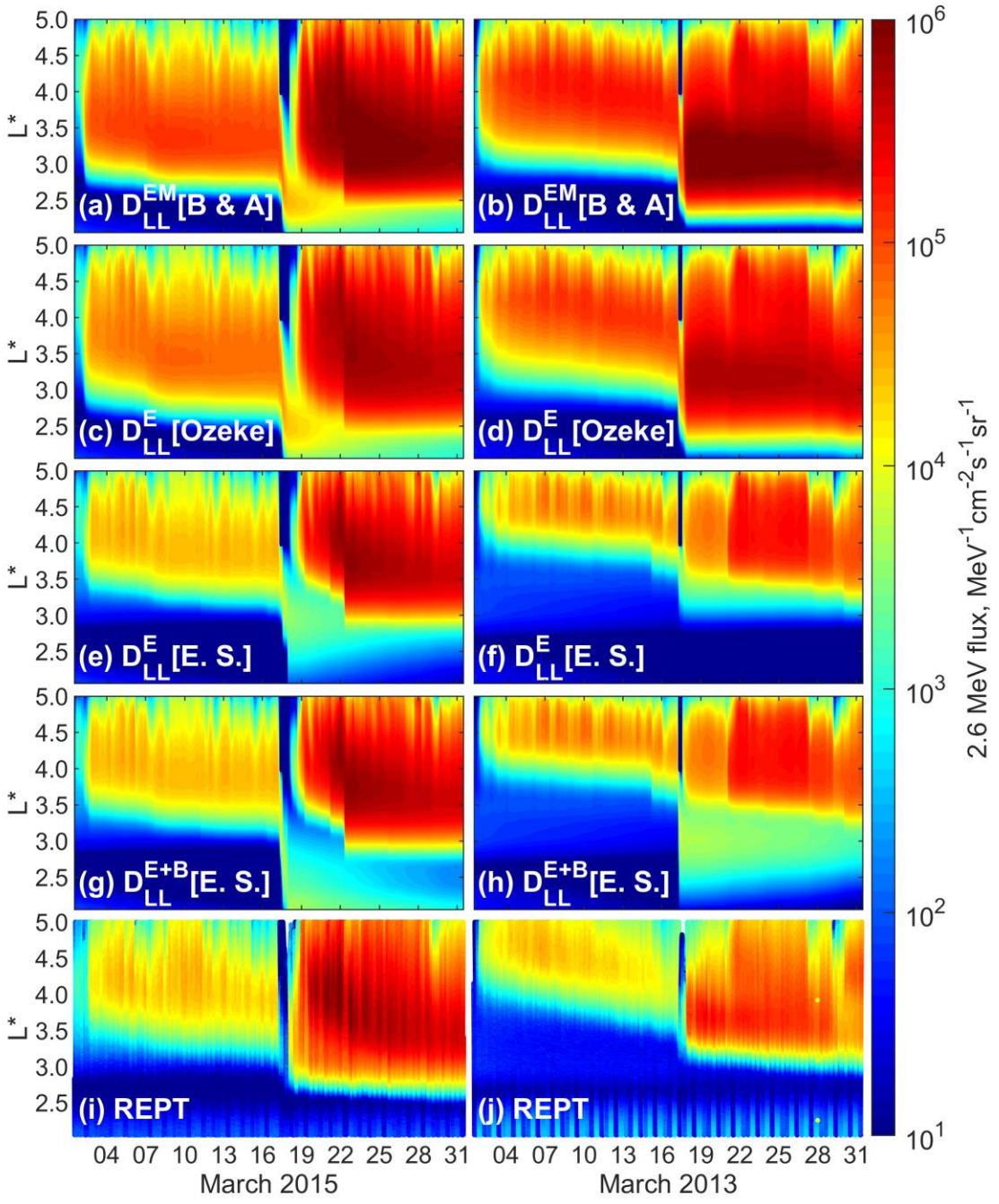

Figure S4: Comparison between the simulated and observed electron flux in the same format as Figure 4 in the main article. Here the during the dropout intervals the electron flux is set to zero at all energies and L-shells down to *L=4.**

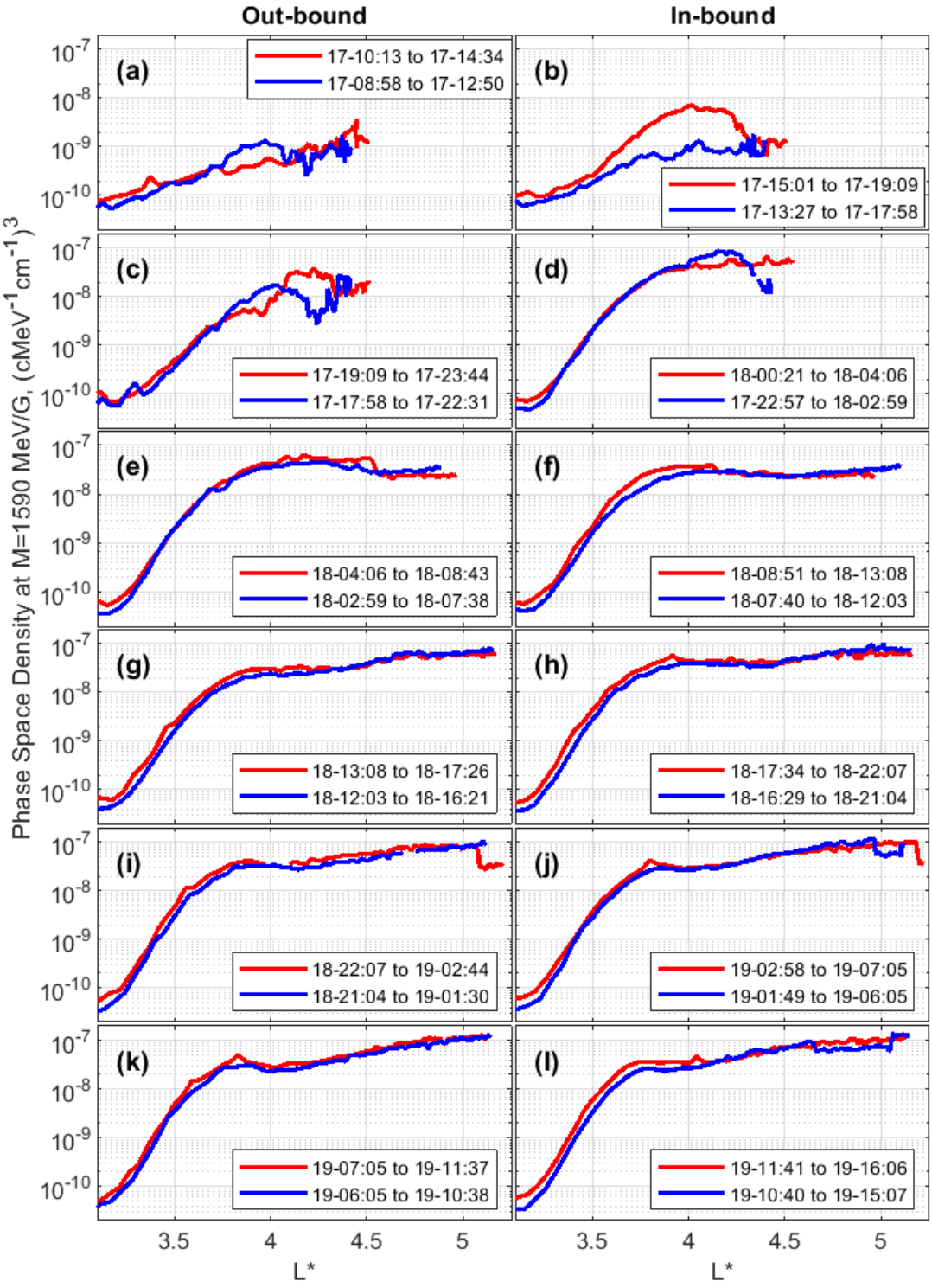

Figure S5: Evolution of the electron phase space density profiles at M=1590 MeV/G and K=0.17 $G^{1/2}Re$ during the March 2013 storm. The red and blue curves represent PSD profiles derived from Van Allan Probes A and B. The start and end times of the out and in bound passes are shown in the legend in the format day-hour:minute.

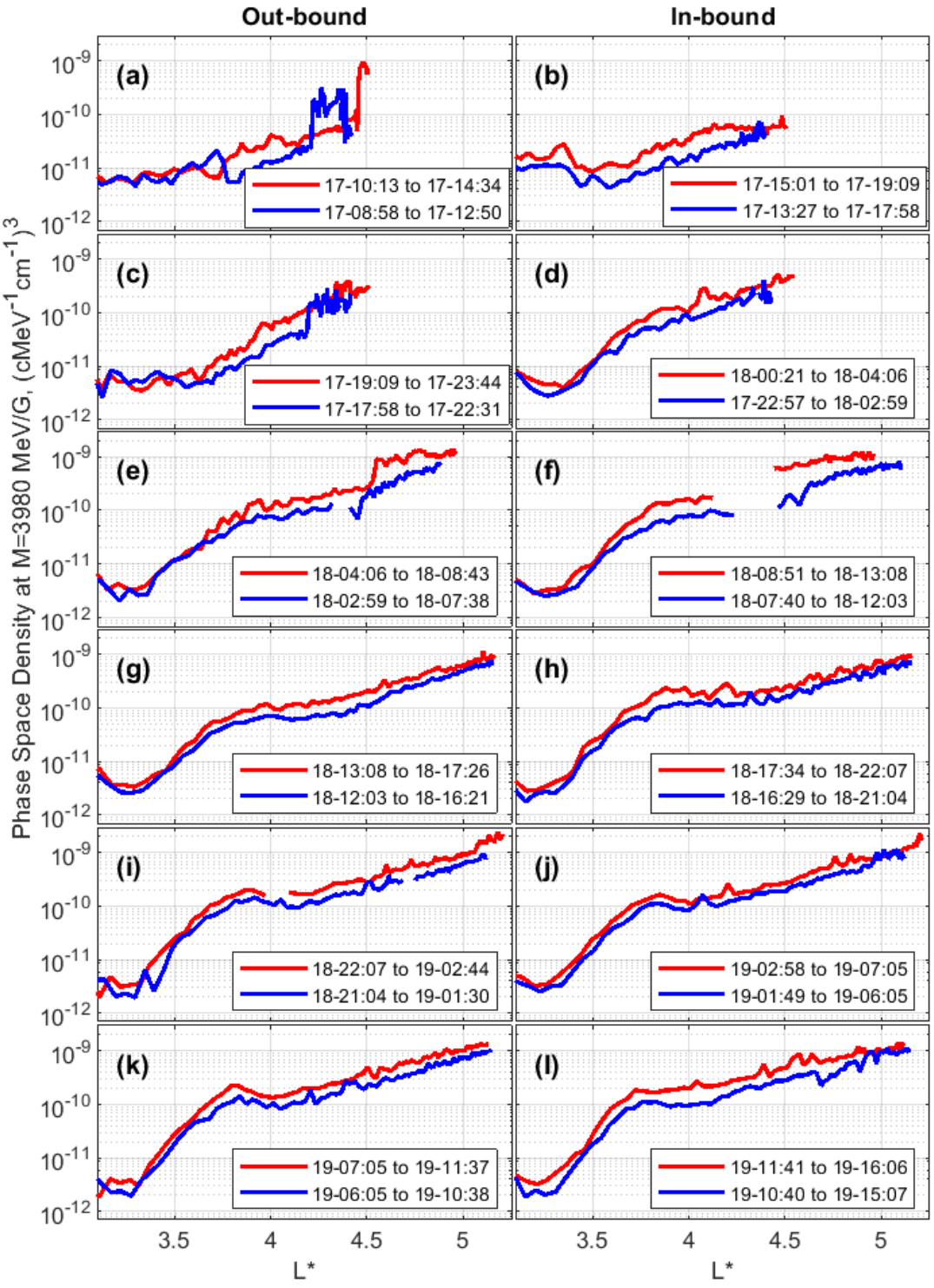

Figure S6: Evolution of the electron phase space density profiles at M=3980 MeV/G and K=0.17 $G^{1/2}$Re during the March 2013 storm. The red and blue curves represent PSD profiles derived from Van Allan Probes A and B. The start and end times of the out and in bound passes are shown in the legend in the format day-hour:minute.